Voltage-Dependent Temperature Coefficient of the *I–V* Curves of Crystalline Silicon Photovoltaic Modules

Yoshihiro Hishikawa, Takuya Doi, Michiya Higa, Kengo Yamagoe, Hironori Ohshima, Takakazu Takenouchi, and Masahiro Yoshita

***Abstract*—The temperature dependence of the *I–V* curves of various kinds of commercial crystalline silicon photovoltaic modules is investigated, based on experiments by using a solar simulator and a thermostatic chamber. The temperature coefficient (TC) of the output voltage of the modules with p-n junction technology is found to closely agree with a formula as a function of their output voltage per cell and temperature, throughout the voltage range of about 0.5–0.7 V per cell, which is important for estimating the P_{max}, fill factor, and V_{oc} of the modules. The formula is derived from a one-diode model, and reproduces the TC of the *I–V* curves within ±5% relative error without adjusting the parameter for each module. The formula is successfully applied for translating the modules' *I–V* curves.**

***Index Terms*—Crystalline silicon, *I–V* curve, p-n junction diode, temperature coefficient (TC), translation.**

I. Introduction

PRECISE understanding of the performance of photovoltaic (PV) devices under various temperature is crucially important, because they operate under a wide range of temperature conditions, whereas their name plate specifications are usually measured at 25 °C. The physical background and practical impact of the temperature-dependent current–voltage (*I–V*) curves of p-n junction PV devices have been extensively investigated since the early stages of their development [1]–[5]. Translation formulas of the *I–V* curves for temperature have been also investigated by many studies [6]–[10]. An international standard on the translation of the *I–V* curves is published [11], and is widely used for industrial purposes. Although the conventional translation procedures are known to have reasonable agreement with experiments [7], [9], [12], [13], they usually require many experimental data in advance. For example, the temperature coefficients (TCs) for the voltage and current in [11] need to be determined by several experimental *I–V* curves for each type of module at preferably each irradiance range [9]. Although the linear interpolation method [10], or the procedure 3 of [11], does not use such parameters, it requires two or more reference *I–V* curves for translation over a wide range of irradiance and temperature conditions.

This study has experimentally investigated the TC of the output voltage of different types of commercial crystalline silicon PV modules at various voltage of the *I–V* curves for the first time. Formula to express the TC is derived based on the one-diode model of p-n junction. Application of the results to practical translation of the *I–V* curves is also discussed.

TABLE I
Experimental Performance Parameters of the PV Modules Used in This Study Under STC

Sample (No. of cells)	I_{SC} (A)	V_{OC} (V)	P_{MAX} (W)	FF (%)	Type
N15A01 (40)	9.18	25.21	177.1	76.5	PV-MA1820LW-1 (Mitsubishi, mono)
N15B05 (48)	9.10	30.22	208.2	75.7	KJ210P-3DD4CG (Kyocera, multi)
N16C03 (72)	6.32	48.3	240.4	78.7	SPR-250NE-WHT-J (Sunpower, mono)
N16D03 (36)	5.56	22.4	94.2	75.5	GT85F (KIS, mono)
SCSI002 (36)	5.26	22.20	85.4	73.2	NT-84L5H (Sharp, mono)
NE-132AR (54)	5.23	32.57	124.4	73.1	NE-132AR (Sharp, multi)
HIP (72)	5.45	51.1	211.5	75.9	HIP-210NKH5 (Sanyo, mono)

Note: The numbers of series-connected cells in the modules are also shown.

II. Experiment

The *I–V* curves of commercial PV modules as shown in Table I were measured at irradiance levels of 0 (dark) and 1 kW/m^2, and temperature levels of 10, 25, 45, and 65 °C by using a large area multijunction module solar simulator (modified WACOM WPSS—2.0 × 1.4) with an illumination area of 2.0 m × 1.4 m, unless otherwise specified. The simulator generates long pulses of light up to about 1 s with irradiance uniformity better than ±1% over the modules' area. Each mea-

Manuscript received July 17, 2017; revised September 12, 2017; accepted October 13, 2017. Date of publication November 28, 2017; date of current version December 20, 2017. This work was supported by New Energy and Industrial Technology Development Organization under Ministry of Economy, Trade and Industry. *(Corresponding author: Yoshihiro Hishikawa.)*

The authors are with the Research Center for Photovoltaics, National Institute of Advanced Industrial Science and Technology, Tsukuba 305-8568, Japan (e-mail: y-hishikawa@aist.go.jp; t.doi@aist.go.jp; m.higa@aist.go.jp; k-yamagoe@aist.go.jp; hironori-ohshima@aist.go.jp; t-takenouchi@aist.go.jp; m-yoshita@aist.go.jp).

Color versions of one or more of the figures in this paper are available online at http://ieeexplore.ieee.org.

Digital Object Identifier 10.1109/JPHOTOV.2017.2766529

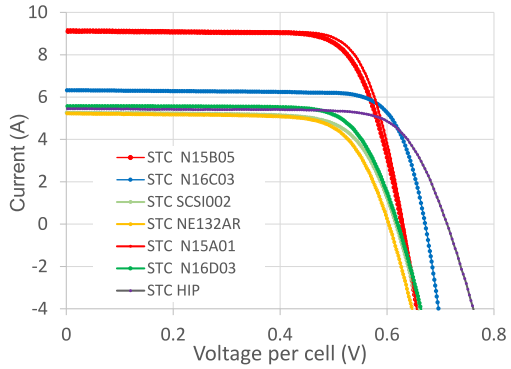

Fig. 1. *I–V* curves per one cell, i.e., the voltage being divided by the series-connected number of cells, of the modules listed in Table I under STC.

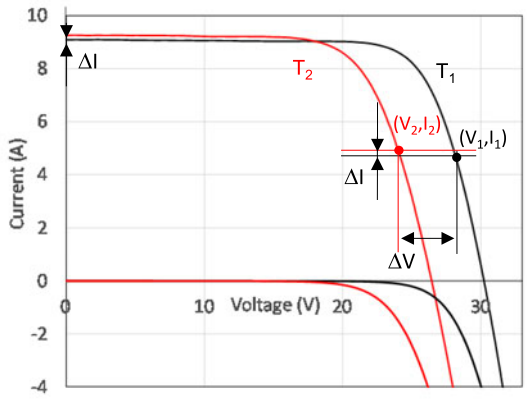

Fig. 2. *I–V* curves of a PV module (N15B05 in Table I) under dark and 1 kW/m^2 at $T_1 = 25$ °C and $T_2 = 65$ °C. Data points (V_1, I_1) and (V_2, I_2) for evaluating the TC are also shown.

surement was carried out within a single pulse. The hysteresis effects of the I-V curves [14]–[16], related to the electrical capacitance of the devices, were avoided by reducing the voltage sweep speed, so that the I-V curves measured under short circuit SC to open circuit OC and OC to SC directions agree [16]. Typical measurement time for each I-V curve was 100–300 ms. The irradiance of the solar simulator was measured and adjusted by using reference PV cells calibrated at AIST. The ambient temperature of the measurement room was kept at about 23 ±1 °C. A thermostatic chamber was used to control the module temperature. When necessary, continuous light of about 150 W/m^2, which was generated by the stand-by operation of the solar simulator, was irradiated on the modules, for finely adjusting the module temperature. Nine Pt100 sensors were attached to the backsheet of the module for monitoring the module temperature. The lateral distribution of the temperature was within ± 0.5 °C and ±1.0 –1.5 °C throughout the module at around 25 °C and other temperatures, respectively, and was confirmed to be stable for more than 30 s before the *I–V* curve measurement. The heating of the module during an *I–V* measurement is estimated to be typically around 0.2–0.3 °C, from the change in $V_{\rm oc}$ under illumination over the measurement window. The average of the nine sensors' readings was used as the module temperature. The irradiance was corrected for the spectral mismatch between the solar simulator and AM1.5G reference solar spectrum [17], taking into account the spectral irradiance of the solar simulator and temperature-dependent spectral response of the modules. Since the samples were crystalline silicon modules, the spectrum-adjustable feature of the simulator was not used in this study.

The measurement reproducibility of the SC current $I_{\rm sc}$, OC-voltage $V_{\rm oc}$, maximum power $P_{\rm max}$, and fill factor (FF) in this study was typically within ±0.3%. The performance of the modules under STC (standard test conditions: irradiance of 1 kW/m^2, spectrum of AM1.5G, and module temperature of 25 °C) [17] are summarized in Table I. Their *I–V* curves per one cell are shown in Fig. 1.

III. Results and Discussion

A. Temperature Coefficient of the I–V Curve

Variation of the output voltage of crystalline silicon PV devices, assuming constant irradiance and output current, was investigated as the TC in this study. Considering the photogenerated current of the module is also dependent on the temperature, typically by about +0.05 %/°C under AM1.5G spectrum, the TC was calculated by the following equation:

$$\mathrm{TC} \equiv \Delta V/(T_2 - T_1) = (V_2 - V_1)/(T_2 - T_1) \qquad (1)$$

so that their difference in the output current $I_2 - I_1$ is equal to the difference in $I_{\rm sc}$ (ΔI), as shown in Fig. 2. Here, the voltages V_1 and V_2 were chosen on the I–V curves at temperatures T_1 and T_2, respectively.

If the effects of series resistance and shunt resistance are negligible, the *I–V* curve of a p-n junction solar cell based on a one-diode model is expressed as [1], [18], [19] follows:

$$I = I_L - I_0 \left[\exp\left(\frac{qV}{kT}\right) - 1\right]. \qquad (2)$$

Here, q, k, T, I_L, and I_0 are the electron charge, Boltzmann's constant, device temperature, photocurrent, and diode saturation current, respectively. The current direction is inverted from that of the references, for adopting to Figs. 1 and 2. The *I–V* curves of practical solar cells can be expressed as follows:

$$I = I_L - I_0 \left[\exp\left(\frac{qV}{nkT}\right) - 1\right]. \qquad (3)$$

Here, n is the diode quality factor, which reflects the carrier recombination dynamics in the solar cell [19]. When the voltage per one cell is larger than about 0.2 V under practical device temperature of 300–350 K, $\exp(qV/nkT) \gg 1$ is satisfied. Considering that the I_0 has temperature dependence expressed as $A\exp(-E_{\rm g}/kT)$ which is related to the product of electron and hole concentrations [19], (3) is rewritten as follows:

$$I \approx I_L - I_0 \exp\left(\frac{qV}{nkT}\right) = I_L - A\exp\left(\frac{qV}{nkT} - \frac{E_g}{kT}\right)$$
$$= I_L - A\exp\left\{\frac{q}{nkT}\left(V - \frac{nE_g}{q}\right)\right\}. \qquad (4)$$

Here, E_g denotes the bandgap energy of silicon. Differentiating (4) assuming constant I_L, I, A, and E_g gives the following:

$$\frac{\partial}{\partial T}\exp\left\{\frac{q}{nkT}\left(V-\frac{nE_g}{q}\right)\right\}=0. \tag{5}$$

$$\therefore \frac{\partial V}{\partial T}=\frac{1}{T}\left(V-\frac{nE_g}{q}\right). \tag{6}$$

It is worthwhile to mention the formulas of previous studies on TC. This study analyzes the TC of the *I–V* curves of various types of commercial PV modules, as functions of the output voltage for the first time. It uses (6), which is similar to the formula of the TC of $V_{\rm oc}$ of solar cells by Green [18], [20]. Fan also theoretically discussed the temperature dependence of $V_{\rm oc}$ [21], by explicitly considering the temperature dependence of A and E_g. Similar formula was also used for analyzing the TC of the forward voltage of light-emitting diodes [22], [23].

This study hereafter uses (6), which is simple and reasonably agrees with experiments by using $nE_{\rm g}$ as an adjustable parameter, as demonstrated below. The assumption of constant I_L and I corresponds to the choice of (V_1, I_1) and (V_2, I_2) in Fig. 2. Equation (6) leads to the following expression of the TC per cell $\mathrm{TC_{cell}}$:

$$\mathrm{TC_{cell}}=\frac{v_2-v_1}{T_2-T_1}=\frac{1}{T_1}\left(v_1-\frac{nE_g}{q}\right). \tag{7}$$

Here, v_1 and v_2 are the output voltages of a cell at temperatures of T_1 and T_2, respectively. Therefore, the TC of a series-connected module assuming constant I_L, or irradiance, and I can be expressed as follows:

$$\mathrm{TC}=\frac{V_2-V_1}{T_2-T_1}=N_c\times\frac{v_2-v_1}{T_2-T_1}$$
$$=\frac{1}{T_1}\left(V_1-\frac{N_c nE_g}{q}\right). \tag{8}$$

Here, V_1 $(=N_{\rm c}v_1)$ and V_2 $(=N_{\rm c}v_2)$ are the output voltages of the module at temperatures of T_1 and T_2, respectively, as shown in Fig. 2. N_c is the number of series-connected cells in the module. Equations (7) and (8) are useful for analyzing the $\mathrm{TC_{cell}}$ and TC of PV devices, and are directly derived from a basic one-diode model, i.e., (3). The product of n and E_g (nE_g) is the only adjustable parameter, since others are directly measurable parameters such as T_1, T_2, V_1, V_2 and fundamental parameters such as q.

Experimental $\mathrm{TC_{cell}}$ of a commercial PV module under 1 kW/m^2 illumination are shown in Fig. 3(a). The product of T_1 and $\mathrm{TC_{cell}}$ is plotted versus v_1, based on the illuminated *I–V* curves measured at various temperature levels around a voltage range of 0.5–0.7 V. The voltage range is important for estimating the OC voltage $V_{\rm oc}$, maximum power $P_{\rm max}$, and FF of the *I–V* curve. The experimental results of $\mathrm{TC_{cell}}$, shown by dots with solid lines, agree well with a calculated result of (7), which is shown by a black dashed line. Here, $nE_{\rm g}/q=1.232$ V was assumed, which corresponds to $E_g=1.12$ eV [19] and $n=1.1$.

The agreement of calculations and experiments demonstrates that the $\mathrm{TC_{cell}}\times T_1$ of the commercial PV module has nearly a linear relation with v_i in a temperature range of 10–65 °C,

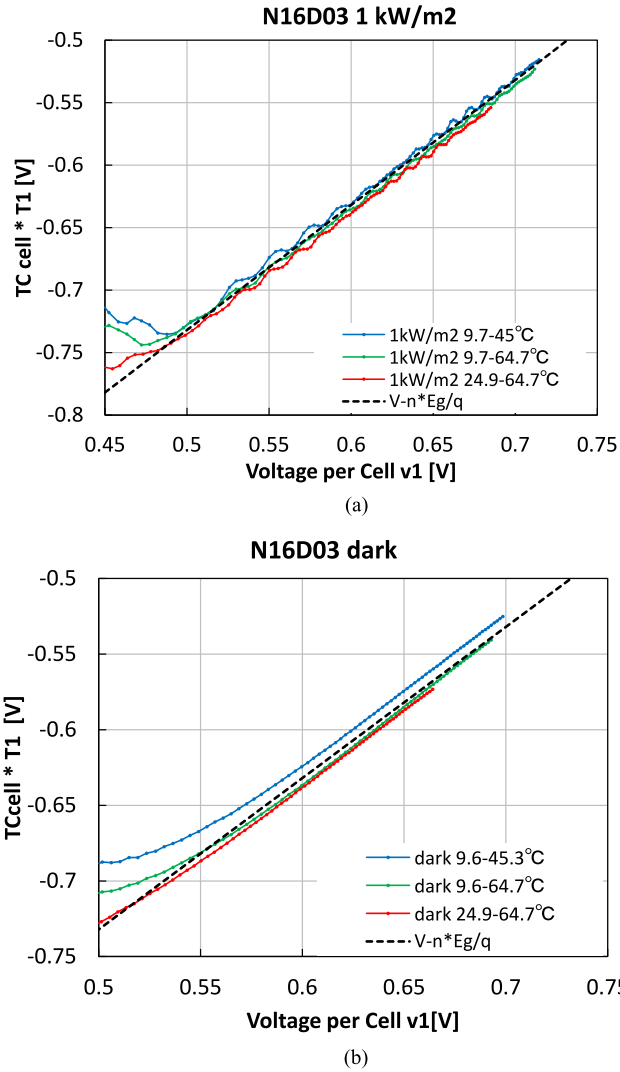

Fig. 3. Typical experimental results of a commercial PV module (N16D03 in Table I). The product of T_1 and $\mathrm{TC_{cell}}$ is plotted versus v_1, based on the experimental (a) 1 kW/m^2 illuminated and (b) dark *I–V* curves at various temperature levels, by dots with solid lines. Calculated result based on (7), with $nE_g/q=1.232$ V, is shown by a black dashed line.

which is expressed by a simple relation of (7). Similar results were also observed under dark conditions as shown in Fig. 3(b). These results suggest that (7) is a good approximation of $\mathrm{TC_{cell}}$ over an irradiance range of 0–1 kW/m^2. There were small discrepancies between the experiment and calculation. For example, the experimental $\mathrm{TC_{cell}}$ showed larger deviation from the calculated results at lower voltages than 0.5 V in Fig. 3(a), and the dark $\mathrm{TC_{cell}}$ was slightly larger than that of 1 kW/m^2. Since the *I–V* curves are affected by the series resistance and shunt resistance as well as the deviation of the *I–V* curve from the one-diode model [19], [24]–[27], they are the possible sources of the deviation. Their dependences on temperature, voltage, and current level are also probably affecting the results. However, this study does not discuss their details, and uses the simple formula of (6), in order to investigate its practical usefulness that the TC can be expressed by minimum number of adjustable parameters.

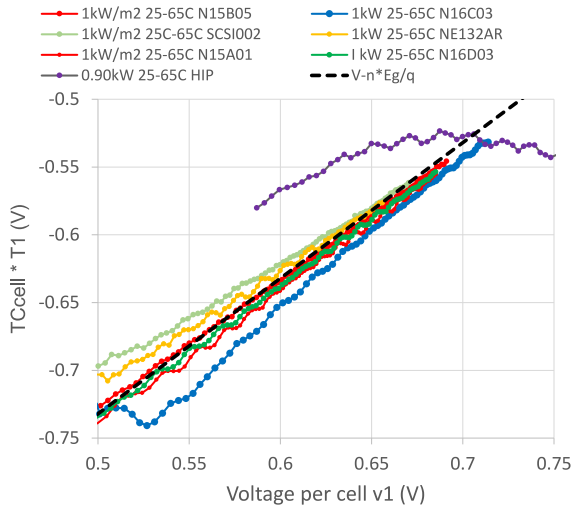

(a)

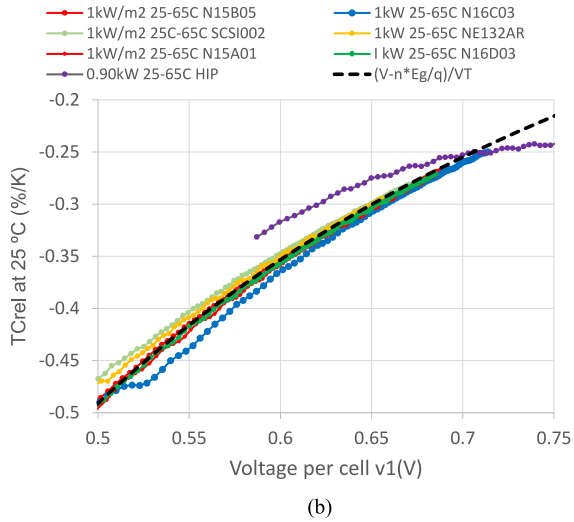

(b)

Fig. 4. (a) Similar results as Fig. 3(a) for various kinds of modules listed in Table I, based on their illuminated *I–V* curves at 25 and 65 °C. (b) Relative temperature coefficient $\mathrm{TC_{rel}}$ of the modules in %/K as expressed in (9), calculated from the same data as (a).

Similar results as Fig. 3(a) for various kinds of modules in Table I are shown in Fig. 4(a), based on their illuminated *I–V* curves in a temperature range of 25–65 °C.

The relation of $\mathrm{TC_{cell}} \times T_1$ and v_1 was similar for most of the modules, and close to the relation of (7) as shown by a black dashed line. The $\mathrm{TC_{cell}}$ was slightly smaller for N16C03, which is a high-performance module based on a backside contact technology. SCSI002 and NE132AR, which are more than 10 years old, with relatively low fill factor and low shunt resistance among the present samples, showed slightly higher $\mathrm{TC_{cell}}$. However, their scatter was small, i.e., within about relative ±5% for the modules in Table I based on crystalline silicon p-n junction technologies. The value of nE_g/q was not optimized for each module, and was fixed to 1.232 V. One module (HIP) showed an exceptionally different result, where the $\mathrm{TC_{cell}} \times T_1$ was higher (i.e., smaller in absolute value) than others at $v_1 <$ 0.7 V, and did not show linear relation with v_1. This is probably because of its different basic cell technology, i.e., the heterojunction of amorphous silicon and crystalline silicon. Precise formulation of TC for those new technology devices is left for further study.

Fig. 4(a) suggests that (7) well describes the $\mathrm{TC_{cell}}$ of various p-n junction-based modules. The practical significance is that it enables to predict the TC with a reasonable accuracy only from one *I–V* curve without additional information. Fig. 4(b) is the relative TC $\mathrm{TC_{rel}}$ in %/K, based on the same data as Fig. 4(a). Calculated result based on (9) is also shown by a black dashed line

$$\mathrm{TC_{rel}} = \frac{1}{V_1}\left(\frac{V_2 - V_1}{T_2 - T_1}\right) = \frac{1}{T_1}\left(1 - \frac{N_c n E_g}{q V_1}\right) = \frac{1}{T_1}\left(1 - \frac{n E_g}{q v_1}\right). \quad (9)$$

The $\mathrm{TC_{rel}}$ is useful for discussing the practical temperature dependence of PV modules. For example, Fig. 4(b) shows that the absolute value of $\mathrm{TC_{rel}}$ is smaller for higher operation voltage per cell v_1. Since higher efficiency modules usually have higher maximum operation voltage, the absolute values of their $\mathrm{TC_{rel}}$ are also usually smaller than those of lower efficiency modules.

B. New Translation Equation of the I–V Curves for Temperature

The present result is readily applicable to the translation of *I–V* curves for temperature. Conventional translation equations [6], [7], which are described as procedure 1 in an IEC standard [11] are as follows:

$$I_2 = I_1 + I_{\mathrm{SC}} \cdot \left(\frac{G_2}{G_1} - 1\right) + \alpha \cdot (T_2 - T_1), \quad (10)$$

$$V_2 = V_1 - R_S \cdot (I_2 - I_1) - \kappa \cdot I_2 \cdot (T_2 - T_1) + \beta \cdot (T_2 - T_1). \quad (11)$$

When we consider translation for temperature at a fixed irradiance, or $G_1 = G_2$, the equations are simplified

$$I_2 = I_1 + \alpha \cdot (T_2 - T_1), \quad (12)$$

$$V_2 = V_1 - \kappa \cdot I_2 \cdot (T_2 - T_1) + \beta \cdot (T_2 - T_1). \quad (13)$$

Here, α, β, and κ are the TC of current, TC of voltage, and curve correction factor, respectively. Those parameters are dependent on the type of the PV module. The $R_{\mathrm{S}}(I_2 - I_1)$ term is omitted in (13), since it is within a few millivolts for the samples and conditions considered in this study, i.e., $G_1 = G_2$ and $|T_1 - T_2| < 50\,^{\circ}\mathrm{C}$. On the other hand, (8) can be rewritten as follows:

$$V_2 = V_1 + (T_2 - T_1) \times \frac{1}{T_1}\left(V_1 - \frac{N_c n E_g}{q}\right). \quad (14)$$

This serves as the translation equation for voltage based on this study. Fig. 5(a) and (b) show results of the translation for the modules listed in Table I from about 25 to 65 °C, by using (14) with $nE_g/q = 1.232\,\mathrm{V}$. Equation (12) was used as the translation for current, and α was assumed to be 0.05%/°C. To be more specific, the following explicit equations were used for

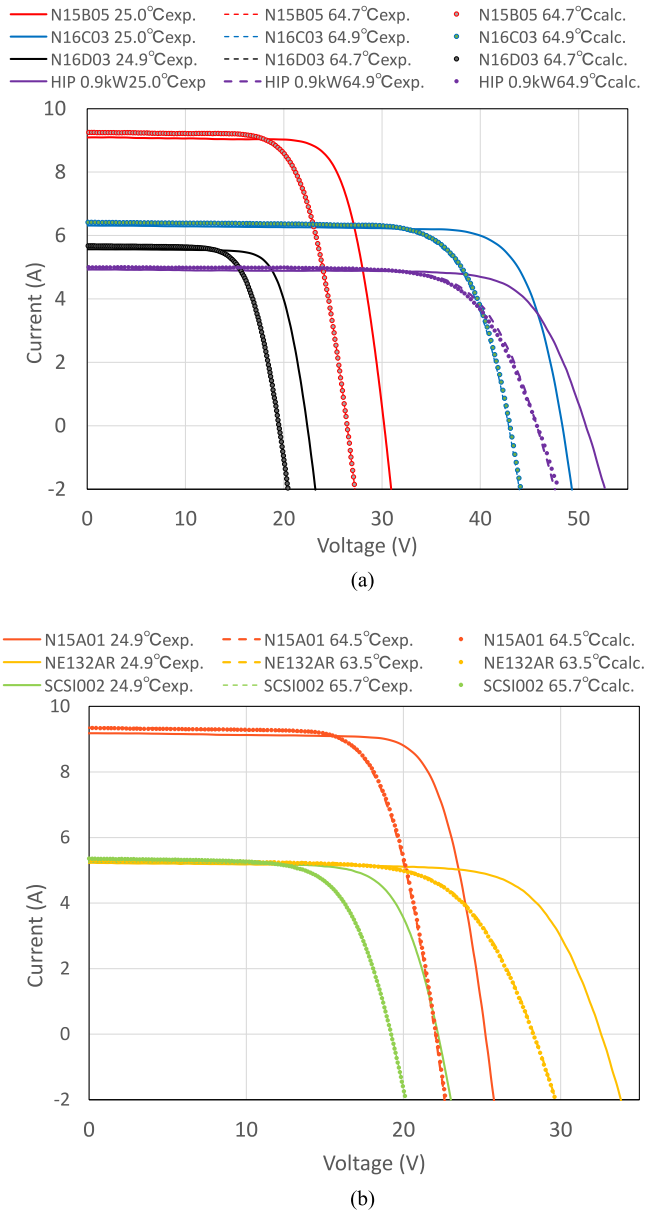

Fig. 5. Results of the translation of the *I–V* curves from about 25 to 65 °C for (a) N15B05, N16C03, N16D03, HIP and (b) N15A01, NE132AR, SCSI002 modules. Calculated results by (15) and (16), are shown by symbols. Experimental results at 25 and 65 °C are shown by solid and dashed lines, respectively.

the translation of the *I–V* curves of all the modules in Fig. 5:

$$I_2 = I_1 + 0.0005 \times I_{\mathrm{sc1}} \left(T_2 - T_1\right), \tag{15}$$

$$V_2 = V_1 + (T_2 - T_1) \times \left[\frac{1}{T_1}\left(V_1 - 1.232 N_c\right)\right]. \tag{16}$$

Here, I_{sc1} is the I_{sc} at T_1. The calculated and experimental *I–V* curves at 65 °C shown by symbols and dashed line in the figure, respectively, agreed very well. Detailed comparison of the experimental I_{sc}, V_{oc}, and P_{max} of the *I–V* curves for the modules listed in Table I are shown in Fig. 6, which agreed

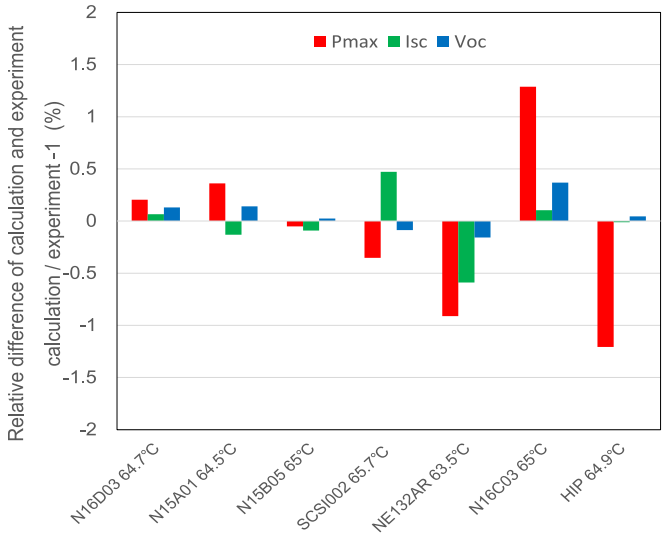

Fig. 6. Relative difference between the experimental I_{sc}, V_{oc}, and P_{max} of the *I–V* curves at about 1 kW/ m^2, 65 °C and calculated results from the curves at 25 °C by (15) and (16).

within about 1% for most of the modules, and within 1.5% for all the modules including HIP, whose $\mathrm{TC}_{\mathrm{cell}}$ deviates from (7) to (9). This indicates that the translation formulas such as (14) and (16) are useful for translating the voltage of the *I–V* curves of the various kinds of PV modules in Table I for temperature. The result suggests that the same translation equation may be used even for a heterojunction module if an error of about 1.5% is allowed, although further experiments by more types of modules are necessary for confirmation.

It is noted that conventional translation equations (12) and (13) also agree very well with experiments in narrow irradiance ranges [9], if the parameters are optimized for each device. For example, comparable or better agreement of V_{oc} and P_{max} with experiments than in Figs. 5 and 6 would be available, if β and κ are chosen to fit the specific temperature and irradiance ranges. However, the value of TC such as β is dependent on the modules types, being affected by the material and structure of the devices [2], [20], [21], [28]. For example, the values of β/V_{oc} of the modules in Fig. 6 range from -0.25% to -0.35%/°C (relative scatter of about $\pm 17\%$) at about 1 kW/ m^2. Therefore, the β should be determined for each module, based on experiments under several temperatures, if conventional translation equations such as (13) is used. For example, [11] describes that the modules' temperature should be changed in steps of approximately 5 °C over a range of at least 30 °C, which means a total of at least seven measurements. On the other hand, the agreement of V_{oc} by the present equations (15)–(16) in Fig. 6 is about $\pm 0.3\%$, which corresponds to the relative difference in the TC of about $\pm 2.5\%$, by using the same value of nE_{g} for all the modules in Table I, and is also applicable to a range of the *I–V* curve around 0.5–0.7 V per cell. The good agreement with experiment is thanks to the formula where the TC is a function of temperature and voltage per cell, based on the basic expression of the *I–V* curves of p-n junction solar cells of (6).

IV. Conclusion

This study has demonstrated that the TC of a crystalline silicon PV module is expressed by (6) not only for $V_{\rm oc}$ but also over a range of the *I–V* curve around 0.5–0.7 V per cell, which is important for estimating the $P_{\rm max}$ and FF of the module, as shown in Fig. 3(a) and (b). It has been also found that the TCs of the output voltage per cell $\rm TC_{cell}$ of various types of commercial PV modules in Table I closely follow the same formula, i.e., (6), with $nE_g/q = 1.232$ V in a voltage range of 0.5–0.7 V per cell, as shown in Fig. 4(a). Its practical significance is that the estimation of TC with reasonable accuracy is possible only from an *I–V* curve and N_c by using (14). The value of nE_g is possibly optimized by further study. Deviation from the formula was also observed for specific types of modules such as high-efficiency heterojunction technology and backside contact technology, although the detail is not investigated in this study.

These results are applied to translation of the *I–V* curves for temperature, as shown in Figs. 5 and 6. Comparison with the experimental $I_{\rm sc}$, $V_{\rm oc}$ and $P_{\rm max}$ (see Fig. 6) showed good agreement within about $\pm 1\%$ for most of the modules, and within $\pm 1.5\%$ for all the modules in Table I. This indicates that the present formula of TC such as (14) and (16) are useful for translating the voltage of the *I–V* curves of PV modules for temperature, especially when the detailed information of their TC is not available.

References

[1] W. Shockley, "The theory of p-n junctions in semiconductors and p-n junction transistors," *Bell Syst. Tech. J.*, vol. 28, no. 3, pp. 435–489, 1949.

[2] M. A. Green, K. Emery, and A. W. Blakers, "Silicon solar cells with reduced temperature sensitivity," *Electron. Lett.*, vol. 2, pp. 97–98, 1982.

[3] J. C. C. Fan, "Theoretical temperature dependence of solar cell parameters," *Sol. Cells*, vol. 17, pp. 309–315, 1986.

[4] A. Louwen, A. C. de Waal, R. E. I. Schropp, A. P. C. Faaij, and W. G. J. H. M. van Sark, "Comprehensive characterization and analysis of PV module performance under real operating conditions," *Prog. Photovolt.*, vol. 25, no. 3, pp. 218–232, 2017.

[5] B. Mihaylov, T. R. Betts, A. Pozza, H. Müllejans, and R. Gottschalg, "Uncertainty estimation of temperature coefficient measurements of PV modules," *IEEE J. Photovolt.*, vol. 6, no. 6, pp. 1554–1563, Nov. 2016.

[6] J. D. Sandstrom, "A method for predicting solar cell current-voltage curve characteristics as a function of incident solar intensity and cell temperature," NASA, Washington, DC, USA, 199-208 JPL Tech. Rep. TR 32-1142, 1967.

[7] W. Herrmann and W. Wiesner, "Current-voltage translation procedure for PV generators in the German 1,000 roofs-programme," in *Proc. Internationales Sonnenforum*, Freiburg, Germany, 1996, pp. 701–705.

[8] B. Marion, S. Rummel, and A. Anderberg, "Current-voltage curve translation by bilinear interpolation," *Prog. Photovolt., Res. Appl.*, vol. 12, pp. 593–607, 2004.

[9] B. C. Duck, C. J. Fell, B. Marion, and K. Emery, "Comparing standard translation methods for predicting photovoltaic energy production," in *Proc. 39th IEEE PVSC*, Tampa, FL, USA, 2013, pp. 0763–0768. doi:10.1109/PVSC.2013.6744261.

[10] Y. Tsuno, Y. Hishikawa, and K. Kurokawa, "Modeling of the *I–V* curves of the PV modules using linear interpolation/ extrapolation," *Sol. Energy Mater. Sol. Cells*, vol. 93, pp. 1070–1073, 2009.

[11] *Photovoltaic Devices—Procedures for Temperature and Irradiance Corrections to Measured I–V Characteristics*, IEC 60891:2009, 2009.

[12] Y. Tsuno and Y. Hishikawa, "Comparison of curve correction procedures for current–voltage characteristics of photovoltaic devices," *Jpn. J. Appl. Phys.*, vol. 51, 2012, Art. no. 10NF02.

[13] K. Paghasian and G. TamizhMani, "Photovoltaic module power rating per IEC 61853–1: A study under natural sunlight," in *Proc. 37th IEEE Photovolt. Spec. Conf.*, 2011, pp. 002322–002327. [Online]. Available: http://www.solarabcs.org

[14] G. Friesen and H. A. Ossenbrink, "Capacitance effects in high-efficiency cells," *Sol. Energy Mater. Sol. Cells*, vol. 48, pp. 77–83, 1997.

[15] J. Metzdorf *et al.*, "Analysis and correction of errors in current-voltage characteristics of solar cells due to transient measurements," in *Proc. 12th Eur. Photovolt. Sol. Energy Conf. Exhib.*, Amsterdam, The Netherlands, 1994, pp. 496–499.

[16] Y. Hishikawa, H. Shimura, and H. Tobita, "Accurate *I–V* curve measurements of high-capacity c-Si solar cells," in *Proc. 28th Eur. Photovolt. Sol. Energy Conf. Exhib.*, Paris, France, 2013, pp. 3159–3162.

[17] *Photovoltaic Devices—Part 3: Measurement Principles for Terrestrial Photovoltaic (PV) Solar Devices With Reference Spectral Irradiance Data*, IEC 60904-3:2016, 2016.

[18] M. A. Green, *Solar Cells*. Englewood Cliffs, NJ, USA: Prentice-Hall, 1982.

[19] S. M. Sze, *Physics of Semiconductor Devices*. New York, NY, USA: Wiley, 1981.

[20] M. A. Green, A. W. Blakers, and C. R. Osterwald, "Characterization of high-efficiency silicon solar cells," *J. Appl. Phys.*, vol. 58, no. 11, pp. 4402–4408, 1985.

[21] J. C. C. Fan, "Theoretical temperature dependence of solar cell parameters," *Sol. Cells*, vol. 17, pp. 309–315, 1986.

[22] Y. Xi and E. F. Schubert, "Junction–temperature measurement in GaN ultraviolet light-emitting diodes using diode forward voltage method," *Appl. Phys. Lett.*, vol. 85, no. 12, pp. 2163–2165, 2004.

[23] D. S. Meyaard *et al.*, "Analysis of the temperature dependence of the forward voltage characteristics of GaInN light-emitting diodes," *Appl. Phys. Lett.*, vol. 103, 2013, Art. no. 121103.

[24] J. Zhao, A. Wang, S. J. Robinson, and M. A. Green, "Reduced temperature coefficients for recent high-performance silicon solar cells," *Prog. Photovolt.*, vol. 4/5, pp. 399–414, 1996.

[25] O. Breitenstein, "Understanding the current-voltage characteristics of industrial crystalline silicon solar cells by considering inhomogeneous current distributions," *Optoelectron. Rev.*, vol. 21, no. 3, pp. 259–282, 2013.

[26] M. Turek, "Current and illumination dependent series resistance of solar cells," *J. Appl. Phys.*, vol. 115, 2014, Art. no. 144503.

[27] K. C. Fong, K. McIntosh, and A. W. Blakers, "Accurate series resistance measurement of solar cells," *Prog. Photovolt.*, vol. 21, no. 4, pp. 399–414, 1996.

[28] S. P.-Alcántaraa *et al.*, "A statistical analysis of the temperature coefficients of industrial silicon solar cells," *Energy Procedia*, vol. 55, pp. 578–588, 2014.

Authors' photographs and biographies not available at the time of publication.